On a geometrical approach in contact mechanics

Alexander Konyukhov, Karl Schweizerhof
Universität Karlsruhe, Institut für Mechanik

Institut für Mechanik
Kaiserstr. 12, Geb. 20.30
76128 Karlsruhe
Tel.: +49 (0) 721/ 608-2071
Fax: +49 (0) 721/ 608-7990
E-Mail: ifm@uni-karlsruhe.de
www.ifm.uni-karlsruhe.de

On a geometrical approach in contact mechanics

Alexander Konyukhov, Karl Schweizerhof

2005

Abstract. The focus of the contribution is on a detailed discussion of the 2D formulation in contact which can be viewed either as a reduction of the general 3D case to a special cylindrical geometry, or as the contact of 2D bodies bounded by plane curves. In addition, typical frictional characteristics, such as the yield surface and the update of the sliding displacements allow a geometrical interpretation in the chosen coordinate system on the contact surface.

1 Geometry and kinematics of contact

In the literature various contact descriptions adapted for an effective finite element implementation are available, which can be characterized by the following: from 2D to 3D formulations, from non-frictional to frictional contact. One of the first contributions on finite element solutions of 2D frictional contact problems based on an elasto-plastic analogy has been made by Wriggers et. al. [1]. General overviews over contact conditions and contact algorithms which are nowadays used in practice, are covered by the books of Wriggers [2] and Laursen [3]. The covariant description, see Konyukhov and Schweizerhof [4] for the frictionless case and [5] for the frictional contact, has been found as a universal penalty based approach for contact with various approximation of the surfaces. In the current contribution, we will show the unity of 2D and 3D formulations, where the 2D case can be derived, from one hand, as a simplified case of the particular 3D geometry of contact surfaces and, from the other hand, can be constructed separately based on the differential geometry of 2D plane curves.

Considering a special contact case – contact between two cylindrical infinite bodies with plane strain deformations, see Fig. 1, leads to the definition of a 2D contact. In this case a generatrix **GH** of the first cylindrical body is a contact line and corresponds to a contact line **G'H'** which is also a generatrix but of the second cylindrical body. Thus, 3D contact which can be seen as an interaction between two surfaces is reduced to an interaction between two boundary curves in the 2D case. One of both boundary curves resp. surfaces is chosen as the master contact curve resp. surface. A coordinate system is considered on the boundary, either for a surface in 3D or for a curve in 2D.

On the plane we define a curvilinear coordinate system associated with the curve by introducing two principal vectors as a basis: the tangent vector $\boldsymbol{\rho}_\xi =$

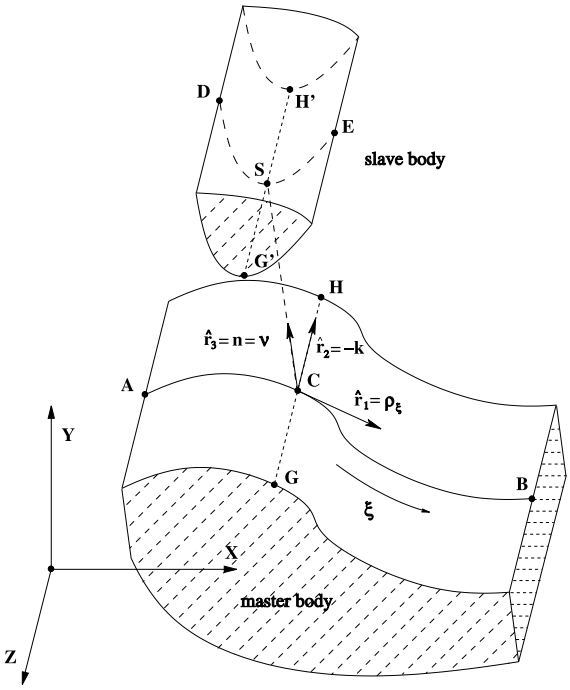

Figure 1: Two dimensional contact as a special case of three dimensional contact

$\frac{\partial \boldsymbol{\rho}}{\partial \xi}$ and the unit normal vector $\boldsymbol{\nu}$. Then a slave contact point $\mathbf{S}$ is found as

$$\mathbf{r}_s(\xi, \zeta) = \boldsymbol{\rho}(\xi) + \zeta \boldsymbol{\nu}(\xi). \tag{1}$$

The normal unit vector $\boldsymbol{\nu}$ in the case of arbitrary Lagrangian parameterizations with ξ can be defined via a cross product in a Cartesian coordinate system as:

$$\boldsymbol{\rho}_\xi = \frac{\partial \boldsymbol{\rho}}{\partial \xi}; \quad \Longrightarrow \quad \boldsymbol{\nu} = \frac{[\mathbf{k} \times \boldsymbol{\rho}_\xi]}{\sqrt{\boldsymbol{\rho}_\xi \cdot \boldsymbol{\rho}_\xi}}, \tag{2}$$

where $\mathbf{k}$ is the third unit vector in this Cartesian coordinate system. According to this definition the traction vector $\mathbf{R}_s$ is defined via the contravariant basis vectors:

$$\mathbf{R}_s = T\boldsymbol{\rho}^1 + N\boldsymbol{\rho}^2 = T\frac{\boldsymbol{\rho}_\xi}{(\boldsymbol{\rho}_\xi \cdot \boldsymbol{\rho}_\xi)} + N\boldsymbol{\nu}. \tag{3}$$

The decomposition of the traction in eqn. (3) leads to the following contact integral

$$\delta W_c = \int_l (N\delta\zeta + T\delta\xi) dl. \tag{4}$$

A closer look reveals that the contact integral (4) contains the work of the contact tractions T and N defined on the master contact curve and is computed along the slave curve $l \equiv l_s$.

2 Regularization of the contact tractions

For the normal traction N, the following regularized equation in the closed form is taken

$$N = \epsilon_N \zeta, \quad if \quad \zeta \leq 0, \tag{5}$$

where ϵ_N is a penalty parameter for the normal interaction.

As a reasonable equation for the regularization of the tangent traction T we choose a proportional relation between the full time derivative $\frac{d\mathbf{T}}{dt}$ and the relative velocity vector expressed in covariant form on the tangent line $\zeta = 0$:

$$\frac{D_1 T}{dt}\boldsymbol{\rho}^1 = -\epsilon_T \dot{\xi}\boldsymbol{\rho}_\xi. \tag{6}$$

Expressing the covariant derivative in eqn. (6) the following equation is obtained

$$\frac{dT}{dt} = -\epsilon_T(\boldsymbol{\rho}_\xi \cdot \boldsymbol{\rho}_\xi)\dot{\xi} + \frac{\boldsymbol{\rho}_{\xi\xi} \cdot \boldsymbol{\rho}_\xi}{(\boldsymbol{\rho}_\xi \cdot \boldsymbol{\rho}_\xi)}\dot{\xi} - \frac{h_{11}}{a_{11}}\dot{\zeta}, \tag{7}$$

where ϵ_T is a penalty parameter for the tangential interaction, a_{11} and h_{11} are components of the metric tensor resp. of the curvature tensor for the cylindrical surface. If a path length $s = \xi$ is used for parameterization, then eqn. (7) is transformed as

$$\frac{dT}{dt} = -\epsilon_T \dot{s} - \kappa\dot{\zeta}, \tag{8}$$

where κ is a curvature of the master contact plane curve.

3 Linearization for a Newton type solution scheme

The derivation of the contact matrices can be performed either according to the cylindrical geometry, or according to the geometry of the plane curves. The latter provides a straightforward geometrical explanation of each part of the contact matrix and can be used for the judgment of their necessity within the solution process. Thus, the linearization of **the normal part** in eqn. (4) given by the following integral:

$$\delta W_c^N = \int_l N\delta\zeta dl, \tag{9}$$

leads to the following.

$$D(\delta W_c^N) = \int_l \left(\frac{dN}{dt}\delta\zeta + N\frac{d\delta\zeta}{dt}\right) dl =$$

$$= \int_l \epsilon_N(\delta\mathbf{r}_s - \delta\boldsymbol{\rho}) \cdot (\boldsymbol{\nu} \otimes \boldsymbol{\nu})(\mathbf{v}_s - \mathbf{v})dl - \tag{10}$$

$$- \int_l \epsilon_N \zeta \left(\delta\boldsymbol{\tau} \cdot (\boldsymbol{\nu} \otimes \boldsymbol{\tau})(\mathbf{v}_s - \mathbf{v}) + (\delta\mathbf{r}_s - \delta\boldsymbol{\rho}) \cdot (\boldsymbol{\tau} \otimes \boldsymbol{\nu}) \frac{\partial \boldsymbol{\tau}}{\partial t} \right) dl - \qquad (10\ a)$$

$$- \int_l \epsilon_N \zeta \kappa (\delta\mathbf{r}_s - \delta\boldsymbol{\rho}) \cdot (\boldsymbol{\tau} \otimes \boldsymbol{\tau})(\mathbf{v}_s - \mathbf{v}) dl. \qquad (10\ b)$$

The form written via the path length allows a simple geometrical interpretation of each part in eqn. (10) and even allows to establish situations where some of the parts are zero. The first part eqn. (10) is called main part and defines the constitutive relation for normal contact conditions. The second part eqn. (10 a) is called rotational part and defines the geometrical stiffness due to the rotation of the tangent vector of the master curve. It disappears when a master segment is moving in parallel, because only in this case the derivative of a unit vector $\boldsymbol{\tau}$ becomes zero. The third part eqn. (10 b) is called curvature part. This part disappears when the curvature κ of a master segment is zero, i.e. in the case of linear approximations of the master segment.

The structure of **the tangential part for the sticking case** is as follows:

$$D_v(\delta W_c^T) = \int_l \left(\frac{dT}{dt} \delta\xi + T \frac{d\delta\xi}{dt} \right) dl =$$

$$- \int_l \varepsilon_T (\delta\mathbf{r}_s - \delta\boldsymbol{\rho}) \cdot (\boldsymbol{\tau} \otimes \boldsymbol{\tau})(\mathbf{v}_s - \mathbf{v}) dl \qquad (11)$$

$$- \int_l T \left[(\delta\mathbf{r}_s - \delta\boldsymbol{\rho}) \cdot (\boldsymbol{\tau} \otimes \boldsymbol{\tau}) \, \frac{\partial \boldsymbol{\tau}}{\partial t} + \delta\boldsymbol{\tau} \cdot (\boldsymbol{\tau} \otimes \boldsymbol{\tau}) \, (\mathbf{v}_s - \mathbf{v}) \right] dl \qquad (11\ a)$$

$$+ \int_l \kappa (\delta\mathbf{r}_s - \delta\boldsymbol{\rho}) \cdot (\boldsymbol{\tau} \otimes \boldsymbol{\nu} + \boldsymbol{\nu} \otimes \boldsymbol{\tau}) \, (\mathbf{v}_s - \mathbf{v}) dl. \qquad (11\ b)$$

Here T is a trial tangent traction computed from the discrete evolution equation (6) at each load step, e.g. under the assumption that the slave point obeys the elastic deformation law.

One can see that the symmetry is preserved for the full sticking case for any curvilinear geometry of the contact bodies.

If sliding is detected, i.e. if $\|\mathbf{T}\| > \mu|N|$, then the sliding force is computed according to Coulomb's friction law within the return-mapping scheme, see [2] and [3]. We also keep a covariant form:

$$T^{sl} = \mu|N| \, \frac{T_{tr}}{\|\mathbf{T}_{tr}\|} = \mu|N| \, (\boldsymbol{\rho}_\xi \cdot \boldsymbol{\rho}_\xi)^{1/2} sgn(T_{tr}). \qquad (12)$$

The linearized contact integral **for the tangential part in the case of sliding** has the same geometrical structure, but contains non-symmetric parts due to the non-associativity of the Coulomb friction law.

Details for the implementation of the linear contact element as well as for the computation according to the return-mapping scheme can be found in Konyukhov and Schweizerhof [7].

4 Treatment of special cases

Some special cases can appear when a direct application of the return-mapping scheme can lead to improper results. The first problem is arising when the applied load is not simply modified proportionally. In this situation a trial load can not be computed only via the evolution equation, because the attraction point ξ^0 must be updated. Thus we have to extend the algorithm as is shown in the following. The second problem is arising when the projection point is crossing an element boundary during the incremental loading. In this case, the computation according to the incremental evolution equation will produce a jump, because the convective coordinate ξ belongs to different elements.

4.1 Update of the sliding displacements in the case of reversible loading

A geometrical interpretation of the trial step in the return-mapping scheme leads to the definition of the elastic region with an attraction point ξ^0

$$|T_{tr}^{(n)}| < \mu |N^{(n)}| \sqrt{a_{11}} \quad \Longrightarrow \quad \epsilon_T |\xi^{(n)} - \xi^0| < \mu |N^{(n)}| \tag{13}$$

If a point $\xi^{(n+1)}$ appears to be outside of the domain at load step $(n+1)$, then its only admissible position is on the boundary of the domain. A sliding force is applied then at the contact point. As long as we have a motion of the contact point only in one direction the sign function for the sliding force $sgn(T_{tr}^{(n+1)}) = sgn(\Delta\xi^{(n+1)})$ does not change and the computation will be correct. However, when a reversible load is applied and it forces the contact point to move forward or backward, the attraction point ξ^0 must be updated in order to define the sign function for the sliding force correctly. This update can be defined geometrically from Fig. 2:

$$|\Delta\xi^{(n+1)}| = |\Delta\xi^{(n+1)}| - \frac{\mu |N^{(n)}|}{\epsilon_T}. \tag{14}$$

Thus, computation of the trial force at the next load step $(n+1)$ has to be made in accordance to the update procedure, see more in Konyukhov and Schweizerhof [7].

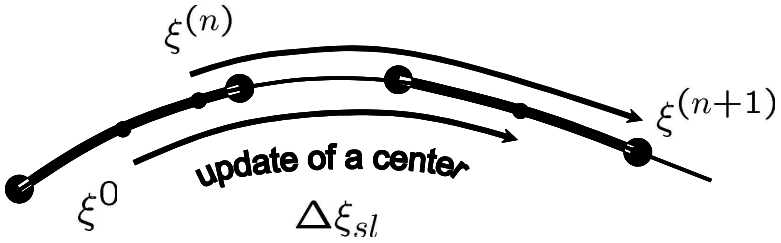

Figure 2: Coulomb friction. Updating of sliding displacements in convective coordinates. Motion of friction cone and center of attraction.

4.2 Crossing an element boundary – continuous integration scheme

Consider two adjacent elements **AB** and **BC**, see Fig. 3. If we follow the computation of the trial force according to the formula expressed in convective coordinates as

$$T_{tr}^{(n+1)} = -\epsilon_T a_{11}(\xi^{(n+1)} - \xi^{(n)}), \tag{15}$$

then this leads to a jump in the contact tractions. The maximum of the jump is computed as

$$T_{jump} = -\epsilon_T a_{11}\left(\lim_{\xi\to -1+0}(\xi)_{\xi\in\mathbf{BC}} - \lim_{\xi\to +1-0}(\xi)_{\xi\in\mathbf{AB}}\right) = 2\epsilon_T a_{11}. \tag{16}$$

This jump appears only due to the different approximation of the adjacent elements. In order to overcome this, we can compute the force in geometrical form. Following this procedure the incremental coordinate $\Delta\xi$ can be expressed as

$$\Delta\xi = \frac{\left(\boldsymbol{\rho}(\xi^{(n+1)})_{\xi\in\mathbf{BC}} - \left(\boldsymbol{\rho}(\xi^{(n)}) + \Delta\mathbf{u}(\xi^{(n)})\right)_{\xi\in\mathbf{AB}}\right)\cdot\boldsymbol{\rho}_\xi^{(n+1)}}{,} a_{11}^{(n+1)} \tag{17}$$

where $\Delta\mathbf{u}$ is an incremental displacement vector. The evolution equation becomes then

$$T_{tr}^{(n+1)} = T^{(n)} - \epsilon_T a_{11}^{(n+1)}\Delta\xi. \tag{18}$$

In the 2D case, the computation can be made via the length parameter s leading to the continuous scheme as well, see Wriggers [2].

5 Numerical examples

5.1 Sliding of a block. Linear approximation of the contact surfaces. Reversible loading process.

We consider the sliding of an elastic block on the rigid base loaded with horizontally prescribed reversible displacements, see Fig. 4(a). The geometrical

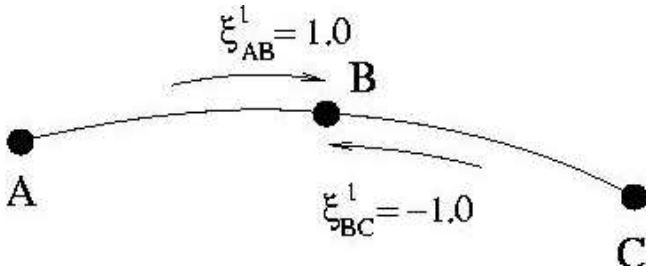

Figure 3: Crossing an element boundary within a load increment. Typical case for the continuous integration scheme.

and mechanical parameters are elasticity modulus $E = 2.1 \cdot 10^4$, Poisson ratio $\nu = 0.3$, length $a = 20$, height $b = 5$, Coulomb friction coefficient $\mu = 0.3$. The penalty parameters are chosen as $\varepsilon_N = \varepsilon_T = 2.1 \cdot 10^6$. The main point is to show the update procedure for sliding displacements. The loading is applied as prescribed displacements at the top side of the deformable block. For contact the "node-to-segment" approach is taken. The hysteresis curve representing the computed horizontal displacement at point **D** vs. the applied displacement at point **C** is given in Fig. 4(b).

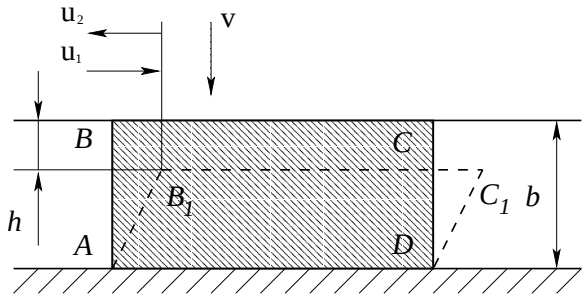

(a) Plane deformation of a block. Applied displacement loading at top of the block.

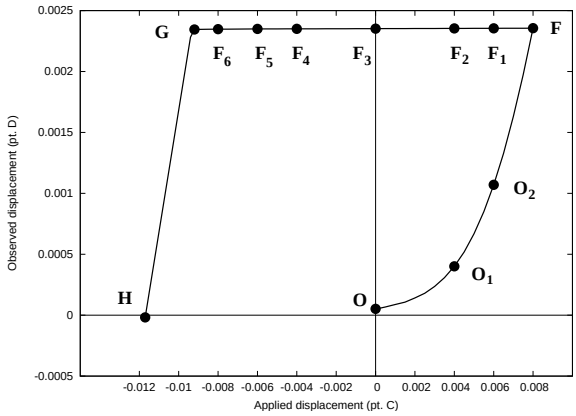

(b) Hysteresis curve. Observed horizontal displacement at point D vs. applied horizontal displacement at point C.

5.2 Drawing of an elastic strip into a channel with sharp corners.

A particular example in which application of the continuous integration is absolutely necessary is a deep drawing of an elastic strip into a channel with sharp corners, see Fig. 4. The crucial point during the analysis is the sliding of a sharp corner **C** over the element boundaries **1**, **2**, **3**. A load-displacement curve computed for the loading point is chosen as the representative parameter to compare various contact approaches. We obtain, see also [7], that the application of the "segment-to-segment" approach, as described in [6], without the

continuous integration scheme allows to compute the force-displacement curve only for non-frictional cases. For frictional cases a more careful transport of the history variables is necessary as it is suggested here.

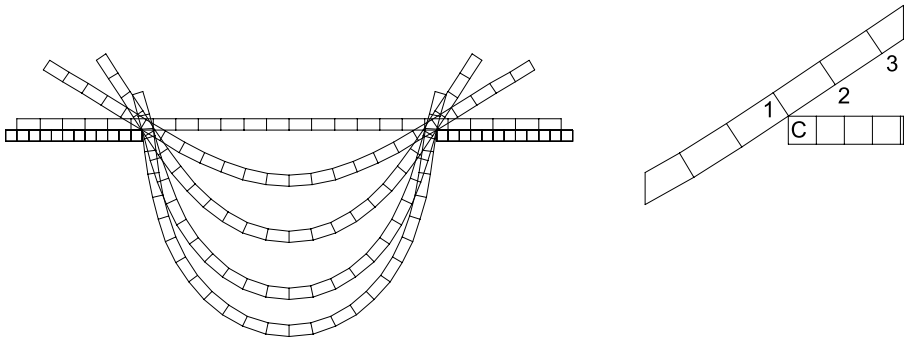

Figure 4: Drawing of an elastic strip into a channel with sharp corners.

6 Conclusions

In this contribution a convective description is reconsidered for the 2D quasi-statical frictional contact problem. Special attention is paid to the derivation of the necessary equations either as a reduction of the known 3D covariant formulation, or directly from the special 2D cylindrical geometry of the contact surfaces. The algorithmic linearization in the covariant form allows to obtain the tangent matrices before the linearization process. Thus, an implementation can be easily carried without providing any special attention to the approximation of the contact surfaces. Further it is shown that special algorithmic techniques have to be taken to provide robust answerers for load reversion and for the crossing of element boundaries.

References

[1] Wriggers P., Vu Van, Stein E. Finite element formulation of large deformation impact-contact problem with friction. *Computers and Structures*, **37**, pp. 319–331, 1990.

[2] Wriggers P. Computational Contact Mechanics. John Wiley & Sons, 2002.

[3] Laursen T. A. Computational contact and impact mechanics. Fundamentals of modeling interfacial phenomena in nonlinear finite element analysis. Springer, 2002.

[4] Konyukhov A., Schweizerhof K. Contact formulation via a velocity description allowing efficiency improvements in frictionless contact analysis. *Computational Mechanics*, **33**, pp. 165–173, 2004.

[5] Konyukhov A., Schweizerhof K. Covariant description for frictional contact problems. *Computational mechanics*, **35**, 3, pp. 190–213, 2005.

[6] Harnau M, Konyukhov A, Schweizerhof K. Algorithmic aspects in large deformation contact analysis using "Solid-Shell" elements. *Computers and Structures*, **83**, 1804–1823, 2005.

[7] Konyukhov A., Schweizerhof K. A special focus on 2D formulations for contact problems using a covariant description. *submitted to International Journal for Numerical Methods in Engineering.*